Article

Shape Effect and Accuracy Analysis of Rock Tensile Strength Test

Junjie Pei, Jinchang Zhao and Shaoqing Niu *

College of Mining Engineering, Taiyuan University of Technology, Taiyuan 030024, China;
peijunjie1254@link.tyut.edu.cn (J.P.); zhaojinchang@tyut.edu.cn (J.Z.)
* Correspondence: niushaoqing@tyut.edu.cn

Featured Application: This paper reveals the influence of the size of disc specimens on the results of splitting tests and provides significant theoretical references for practical experiments. It proposes correlation coefficients for the tensile strength of specimens with different shapes and quantifies the correction method for actual tensile strength. The applicability of different specimen shapes is compared, highlighting the advantages of disc specimens in engineering practice.

Abstract: To investigate the influence of shape effects on the tensile strength of rocks, splitting tests were conducted on disc specimens with the same thickness-to-diameter ratio but different diameters using physical similarity simulation and numerical simulation experiments. Additionally, finite element analysis software was employed to perform numerical simulation tests on two types of dumbbell-shaped specimens involved in direct tensile tests of rocks. This study revealed that when the thickness-to-diameter ratio is fixed at 0.5, the splitting tensile strength decreases gradually as the specimen diameter increases from 30 mm to 110 mm. This trend can be well fitted using a power function. The tensile strength measured from direct tensile tests on the two types of dumbbell-shaped specimens shows a slight decreasing trend as the diameter of the central effective test area decreases. Moreover, the measured tensile strength is lower than the actual tensile strength. The test results for disc specimens are the closest to the actual tensile strength, followed by arc-transition dumbbell-shaped specimens, and lastly, straight-transition dumbbell-shaped specimens. The correlation coefficients between the test results and the actual tensile strength for the three types of specimens are also provided.

Keywords: tensile strength; thickness-to-diameter ratio shape effect; diameter; dumbbell specimen; accuracy comparison

1. Introduction

Tensile strength, as one of the basic mechanical indicators of rocks, has significant implications for the design of rock engineering structures and stability control in underground engineering construction [1]. Currently, the methods for determining the tensile strength of rocks are generally classified into direct and indirect measurements [2]. Direct measurement involves direct tensile tests on rocks. The tensile strength values determined by direct tensile tests are the closest to the true tensile strength of rocks [3,4]. However, due to the typical brittle nature of rocks, conducting direct tensile tests in the laboratory is rather challenging [5–7]. Indirect measurement methods mainly include the Brazilian splitting test and the three-point bending test [8], among which the Brazilian splitting

method is widely used in engineering to determine the tensile strength of rocks because of its convenient specimen preparation and strong operability of the test [9,10].

A significant number of studies conducted (both domestically and internationally) have focused on accurately measuring the tensile strength of rocks, as well as comparing various measurement methods. These studies have yielded many valuable results. In terms of measuring rock tensile strength, researchers Matthew A. Perras and Mark S. Diederichs [11] proposed a conceptual model based on brittle spalling. They determined the tensile strength of rocks using the damage initiation threshold method. Their findings indicated that the results obtained from the Brazilian splitting test (BTS) often overestimate the true tensile strength (DTS). To address this, they proposed correction factors specific to different rock types: 0.9 for metamorphic rocks, 0.8 for igneous rocks, and 0.7 for sedimentary rocks. Furthermore, D. Vogler [12] introduced an innovative idea for measuring tensile strength by using three-dimensional images of the rock fracture surface. This indirect measurement method represents a new direction in testing technology. In the realm of direct tensile tests, Eren Komurlu [13] designed a new loading apparatus that incorporates an insertable disc drill hole rod to measure the direct tensile strength of rocks. He investigated the ideal contact angle between the rock and the loading rod, recommending a contact angle of 50° as optimal. Additionally, he examined how specimen shape affects test results and offered suggestions for optimization. Regarding the Brazilian splitting test method, You Mingqing, Huang Yaoguang, and their colleagues [14–16] conducted indoor experiments and theoretical analyses to assess the impact of loading angles on test results. They concluded that a platform loading angle between 20° and 30° could yield more accurate measurements of tensile strength. In summary, the existing research has provided substantial theoretical and technical support for improving the measurement methods of rock tensile strength across various aspects. Through comparative analyses of direct tensile tests and Brazilian splitting tests, scholars have proposed correlation coefficients and correction factors between different methods, as well as optimized specimen designs and loading techniques. These findings lay crucial groundwork for further enhancing the accuracy and practicality of rock tensile strength testing.

However, current research on splitting tests mainly focuses on the relationship between the height-to-diameter ratio of disc specimens and their tensile strength, with little attention given to the size effect of the disc diameter [17]. Given the general lack of systematic studies on the effects of specimen shape and size in existing research, especially the absence of an in-depth comparison of the correlation between tensile strength results obtained by direct tension and platform splitting tests, this study combines laboratory experiments with numerical simulations to comprehensively analyze the shape effects of various testing methods. Additionally, it focuses on comparing the accuracy and correlation of tensile strength results from two different shaped specimens under the direct tension method and disc specimens in platform splitting tests. This research not only provides new insights into the mechanical mechanisms reflected by specimens of different shapes and sizes in determining rock tensile strength but also offers valuable guidance for selecting appropriate specimen shapes and sizes in engineering practices to obtain more reliable experimental results.

2. Analysis of Shape Effects in Splitting Tests

2.1. Similitude Simulation Test

To (rigorously) analyze the shape effects caused by the disc diameter in splitting tests, this study first considers the complexities of core sampling in real engineering practices. During field core drilling, due to the inherent heterogeneity of rock, even different parts of the same rock layer or block may exhibit significant variations in mechanical proper-

ties, particularly in rock strength. This heterogeneity can interfere with the accuracy and reliability of subsequent experimental data. Therefore, to minimize the impact of uncontrollable factors and ensure the comparability of experimental data, this study employs similar simulation materials. Cement, river sand, and water are mixed in a ratio of 1:3:0.7 to prepare rock-like materials, enabling shape effect analysis under controlled laboratory conditions, thereby overcoming the inherent inconsistencies of natural rock samples.

According to the "Standard of Engineering Rock Mass Testing Methods", this experiment selected disc specimens with a thickness-to-diameter ratio of 0.5. To systematically investigate the impact of shape effects on splitting test results, the disc diameters in the numerical model were set to 30, 40, 50, 70, 90, and 110 mm. These specimens cover a range of diameters from small to large, which facilitates a thorough investigation of the influence of disc diameter on the splitting test results. The thickness-to-diameter ratio of the specimens was uniformly set to 0.5 [18]. Eight specimens of each diameter were produced, yielding a total of forty-eight specimens. This large sample design enhances the representativeness and statistical reliability of the experiment. After production, all specimens underwent a 28-day standard curing process to ensure that the strength of the similar materials stabilized. The splitting tests were then performed on these disc specimens, as shown in Figure 1, to quantitatively analyze the impact of disc diameter on shape effects.
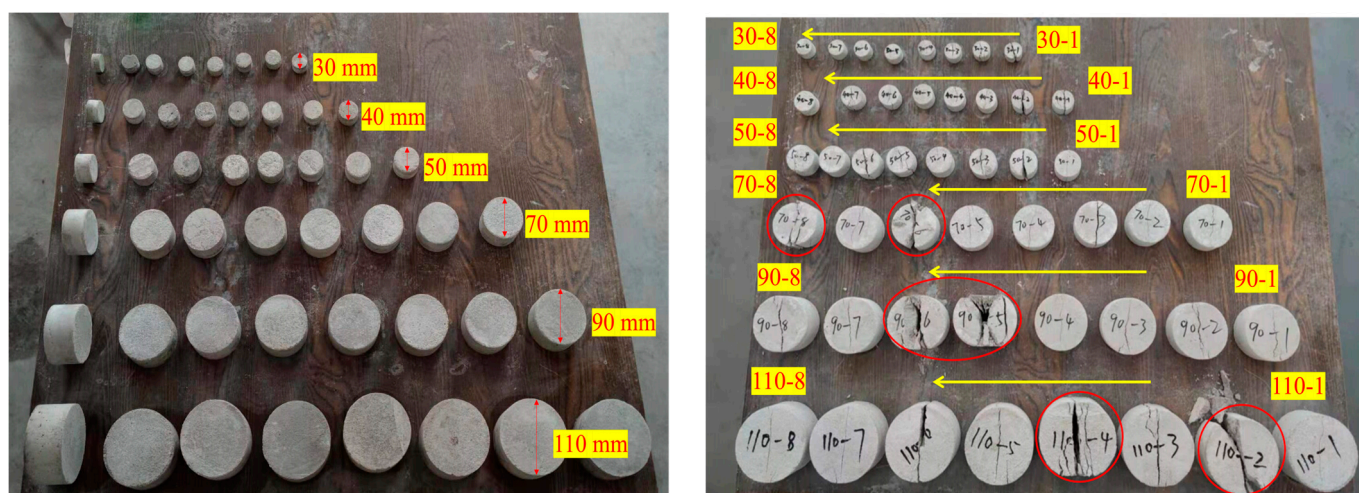

Figure 1. Split test disc specimen (**left**) and split result (**right**).

2.2. Splitting Test Results

The obtained load–displacement curve is shown in Figure 2. The basic mechanical parameters of rock-like materials are shown in Table 1.

Table 1. Basic mechanical parameters of rocks.

Density (g·cm^{-3})	Porosity (%)	P-Wave Velocity (m·s^{-1})	Elastic Modulus (GPa)	Cohesion (MPa)	Internal Friction Angle (°)	Poisson's Ratio	Uniaxial Compressive Strength (MPa)
2.3	20	3800	25	2	30	0.2	30
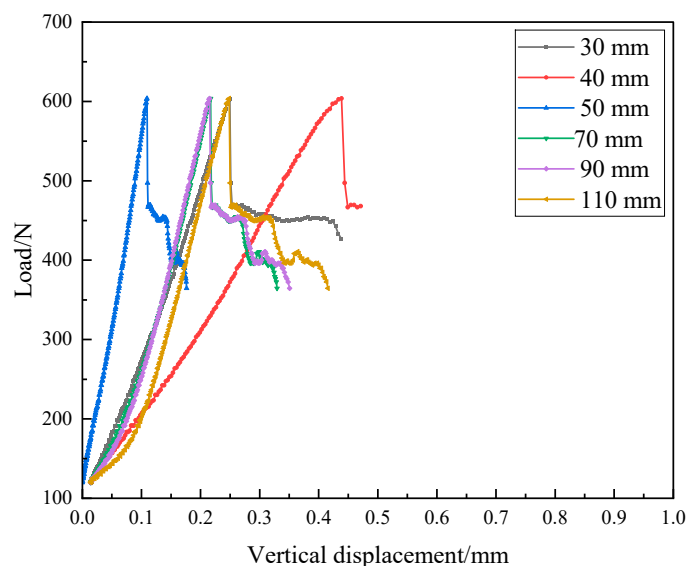
Figure 2. Splitting load–displacement curve.

By analyzing the load–displacement curve after the specimen splitting, it was found that the specimen exhibited good elastic characteristics with increasing pressure in the initial stage, which corresponds to the compaction stage. However, once the strength reaches its peak, the stress rapidly drops with almost no residual strength, exhibiting characteristics of brittle failure. Additionally, upon observing the fractured specimen, the cracks were found to propagate radially and gradually extended to the specimen's edge. This is due to the rapid propagation of the cracks without significant plastic deformation, which is typical of brittle fracture behaviour [19].

The calculation of the splitting tensile strength is based on Equation (1) [20,21]:

$$\sigma_t = \frac{2P}{\pi Dt} \tag{1}$$

In the equation, P represents the maximum pressure at the point of splitting failure of the specimen, in units of N; D is the diameter of the disc specimen, in metres; and t is the thickness of the disc specimen, in metres. The tensile strength of the disc specimens in this similar simulation experiment, calculated using the above equation, is shown in Table 1.

Some data in Table 2 show that the specimens exhibited poor fragmentation, and the actual failure surface deviated from the centreline of the specimen diameter (as indicated by the red circle in Figure 1 (right)). The measured tensile strength deviated significantly, making it unsuitable for use as valid experimental data, and was thus discarded. The data in Table 1 show that the standard deviation for each group is small, indicating low dispersion and high accuracy. This also confirms that, compared to field core sampling, the tensile strength of specimens made using similar material preparation techniques in the laboratory exhibits greater accuracy and consistency. Based on the average tensile strength values obtained from the experiments in Table 2, as the specimen diameter increases from 30 mm to 100 mm, the measured strength decreases by 17.17%, 27.27%, 31.31%, 44.44%, and 51.52%, respectively. This phenomenon is caused by the differing internal stress distributions in specimens of varying sizes. It is evident that the size effect of the specimen diameter on the test results cannot be ignored in the splitting test.

Table 2. Similar simulation test results.

Diameter (mm)	Test 1	Test 2	Test 3	Test 4	Test 5	Test 6	Test 7	Test 8	Standard Deviation	Average Value
30	0.87	Failed	Failed	Failed	0.90	1.07	1.08	1.03	0.08 9	0.99
40	0.79	0.85	0.85	0.76	0.84	0.83	0.70	0.95	0.06 7	0.82
50	0.88	0.63	Failed	0.83	Failed	0.66	0.74	0.59	0.10 4	0.72
70	0.67	0.72	0.70	0.75	0.67	Failed	0.58	Failed	0.05 4	0.68
90	0.49	0.48	0.56	0.50	Failed	Failed	0.64	0.60	0.05 8	0.55
110	0.55	Failed	0.41	Failed	0.52	0.54	0.41	0.43	0.06 0	0.48

2.3. Numerical Simulation Validation

This study systematically analyzes the shape effects caused by disc diameter by conducting similar simulation experiments in the laboratory, coupled with numerical simulations of disc specimens using the finite element analysis software ANSYS 19.0. The finite element method is widely applied in engineering mechanics, particularly in the analysis of complex loads and geometries, where it demonstrates significant advantages. Compared to traditional physical experiments, numerical simulations not only provide precise stress field distributions but also reveal the micro-mechanisms of material failure, without being constrained by physical testing conditions. Therefore, the numerical simulations using ANSYS software not only provide theoretical support for the experimental data but also offer insights into the in-depth analysis of the influence of disc diameter on shape effects.

The material dimensions selected in the numerical simulation validation are the same as those in the similitude simulation test. The material was selected from the ANSYS material library, with a tensile strength of $\sigma_t = 5$ MPa. These material parameters meet the conventional experimental requirements in engineering rock mechanics and effectively simulate the stress response and failure modes of rock-like materials during the splitting process. However, due to limitations in processing accuracy during actual tests, the contact between the plate and the disc may not always remain perfectly tight [22]. This incomplete local contact may lead to stress concentration effects, thereby affecting the precision of the test results. Furthermore, the unique loading method of the test means that the traditional line load model may not fully reflect the actual failure conditions on the disc surface. Therefore, based on existing academic research, this study adopts a 20° curved surface loading method for numerical simulations [14], aiming to more accurately simulate the effect of actual loading conditions on disc failure, as shown in Figure 3. The curved surface loading method effectively simulates the nonlinear stress distribution between contact surfaces, avoiding potential stress calculation deviations that may arise from traditional methods.
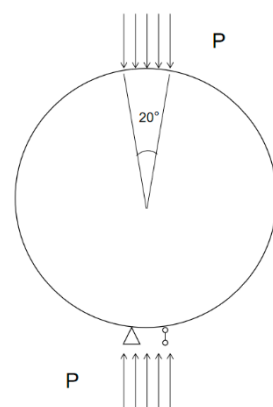
Figure 3. Loading method.

2.4. Experimental Analysis

The data in the table were plotted as scatter points and fitted using a power function, as shown in Figure 4a. The average values of the six groups of tensile strength data were then calculated and fitted again using a power function, resulting in a curve with a higher goodness of fit, as shown in Figure 4b. A comparison with the fitted curve of the numerical simulation results in Figure 4c shows that the results from the laboratory material simulation and the numerical simulation are very similar. In the numerical simulation results, the decrease in strength with decreasing diameter is less pronounced than in the laboratory tests, because the numerical model is based on homogeneous materials [23], which differs from the actual conditions.
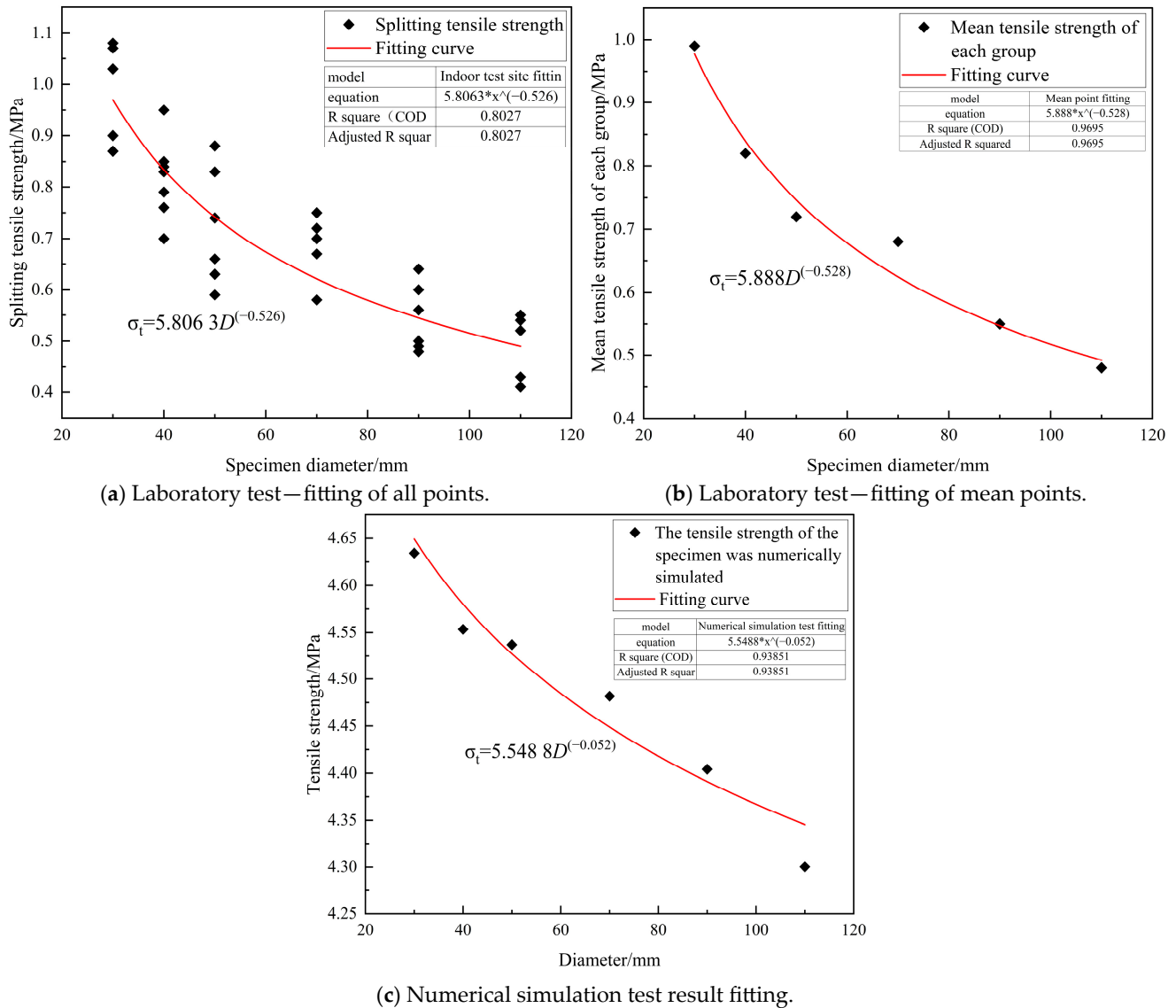

(**a**) Laboratory test—fitting of all points.

(**b**) Laboratory test—fitting of mean points.

(**c**) Numerical simulation test result fitting.

**Figure 4.** Relationship between tensile strength and disc diameter.

The results above indicate that in the splitting test, with the thickness-to-diameter ratio fixed at 0.5, the measured splitting tensile strength decreases as the disc diameter increases, and the deviation from the true strength gradually increases. This trend can be well fitted using a power function.

3. Comparison and Analysis of the Accuracy Between Direct Tension and Brazilian Splitting Tests

3.1. Test Scheme

3.1.1. Numerical Simulation Test Specimen

First, a standard direct tensile specimen of 50 mm (Diameter) × 100 mm (Height) is established for comparison [24], as shown in Figure 5a. For the specimens used to measure rock tensile strength in this numerical simulation test, a model as shown in Figure 5 is established. Specifically, the specimen in Figure 5b is referred to as the curved-transition surface dumbbell specimen, the specimen in Figure 4c is referred to as the straight-transition surface dumbbell specimen, and the specimen in Figure 5d is a disc specimen. The centre effective test area of both dumbbell specimens has a height-to-diameter ratio of 2:1. The radius of the curved-transition surface in the curved-transition dumbbell specimen is approximately (1~2) × d [2], where d is the diameter of the standard cylindrical specimen, as described by Matthew A. Perras et al. In this numerical simulation test, the transition surface radius is taken as 50 mm, and the transition angle of the straight-transition dumbbell specimen is set at 63° [25]. The stress distribution in samples with a 63° angle can be practically accepted as uniaxial. Additionally, no holding or fixing issues were observed in tests on both soft and hard rock materials. This angle is evaluated as the most ideal geometric shape for obtaining accurate results for various rock materials and is more suitable for assessing direct tensile strength, as shown in Figure 5c. Compared to the standard cylindrical tensile specimen shown in Figure 5a, the transition surface of the dumbbell specimen effectively eliminates the stress concentration at the ends caused by loading during direct tensile testing. This results in a more manageable stress distribution and significantly reduces the occurrence of invalid failure in regions far from the specimen's centre [5,26,27]. Additionally, the dumbbell specimens are easy to clamp during laboratory tests, as shown by ① and ② in Figure 5b,c. The curved-transition dumbbell specimen can have the clamps directly mechanically held at the vertical edges of the "dumbbell" ends, or at the edges of the transition surface. Similarly, the straight-transition dumbbell specimen can be simply clamped at the vertical edges of both ends of the specimen, or directly at the transition surface [28,29].
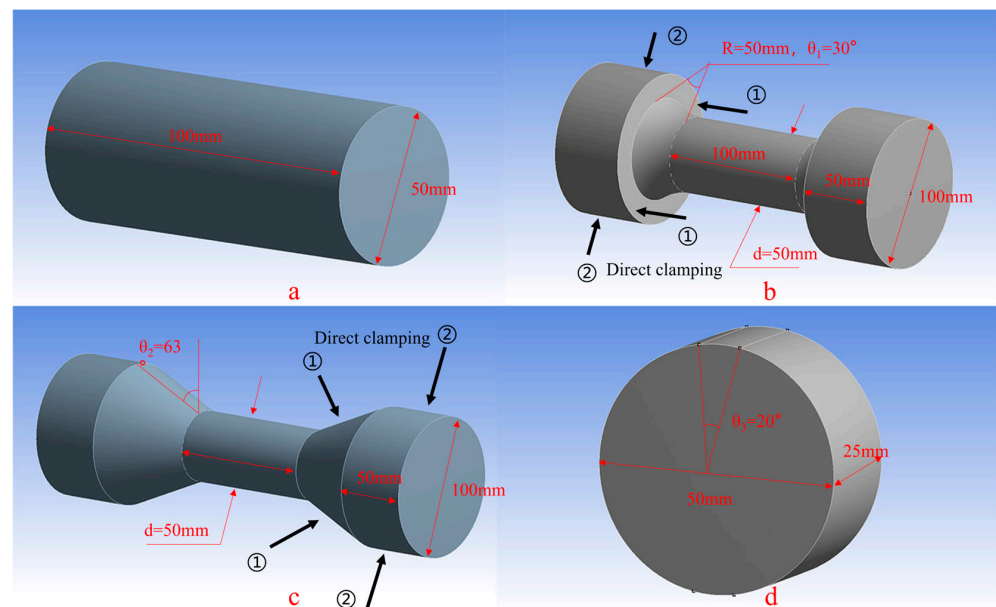
Figure 5. Numerical simulation test specimen. (**a**) Direct tensile standard specimen; (**b**) Dumbbell-shaped specimen with curved-transition surface; (**c**) Dumbbell specimen with linear-transition surface; (**d**) Brazilian disc specimen.

3.1.2. Parameter Selection

Based on different specimen shapes, specimens with various diameters were established to study the effects of shape and size on the tensile strength of rocks. The selected test material has a compressive strength of 50 MPa and a tensile strength of 5 MPa. The elastic modulus of the experimental material is E = 10 GPa, the Poisson's ratio is ν = 0.18, and the density is ρ = 2.3 g/cm^3. In practical research, numerical simulations often use homogeneous material models, while the rock materials in actual experiments are heterogeneous. To more accurately reflect the experimental results, we adopted model microparameters in the numerical simulation that closely resemble the mechanical properties of the experimental materials. Additionally, parameter calibration was performed to ensure the consistency of the simulation results with experimental data. By controlling parameters, we aimed to make the simulated test conditions as close as possible to the actual experimental conditions, thereby ensuring the accuracy of the numerical simulation results. The calibrated model microparameters are shown in Table 3. The mesh was divided using tetrahedral elements, with a unit size of 2 mm. The elastic modulus of the model is assumed to be the same in tension and compression, and the simulated material is defined as a linear elastic material. In field tests, whether drilling rock cores or processing dumbbell-shaped specimens, the diameter of the specimens will have some error. To simulate real-world conditions, the experimental plan is arranged as shown in Table 4.

Table 3. Micro-properties of rock in numerical simulation.

Density ρ (g·cm^{-3})	Fracture Toughness K_{IC} (MPa·m$^{0.5}$)	Crack Friction Factor k	Crack Cohesion c_f (MPa)	Porosity n (%)	Damage Evolution Parameter	Mohr–Coulomb Friction Parameter
2.3	0.8	0.4	2	20	1	0.6

Table 4. Test plan arrangement.

Specimen Shape	Diameter Range/mm
Dumbbell-shaped specimen with curved-transition surface	45~55
Dumbbell specimen with linear-transition surface	45~55

Note: Take one piece for every 1 mm in diameter.

For the three types of direct tensile specimens, the Z-axis is the centreline of the model. The boundary conditions are as follows: one end face has no displacement along the Z-axis, and the centre point of this end face has no displacement in the X, Y, or Z directions. A force load is applied to the opposite end face.

3.2. Test Results and Analysis

For the standard cylindrical specimens, during the field tests, the uneven attachment of the loading blocks on both ends leads to stress concentration on the end faces during loading, resulting in eccentric errors. In contrast, no such errors exist in the numerical simulation; thus, the direct tensile tests of the standard cylindrical specimens are not further analyzed. The standard tensile strength values presented below are derived from the results of the tensile tests of the simulated standard cylindrical specimens [1,30–34].

Figure 6 presents the results of the numerical simulation of disc splitting, including stress distribution contour maps at different time points for the disc's end face and the Y-Z cross-section. As shown in the figure, ignoring the stress concentration effect at the loading point, the maximum tensile stress initially occurs at the centre of the disc's end face. This is because, during the loading process, the centre of the disc's end face experiences the most concentrated stress due to the loading effect. This position is a potential initiation site

for cracks. Subsequently, the region of maximum tensile stress expands from the centre of the cross-section along the Y-axis toward the loading point, ultimately resulting in a spindle-shaped stress distribution. The stress distribution contour map of the Y-Z cross-section shows that the maximum tensile stress region of the disc extends from the centre of the end face along the Z-axis toward the specimen centre, i.e., the origin of the spatial coordinates. Based on the above analysis, it can be concluded that the crack initiation point of the disc-splitting test is at the centre of the cross-section, with the crack subsequently expanding toward the loading point and the specimen centre, ultimately penetrating the entire specimen.
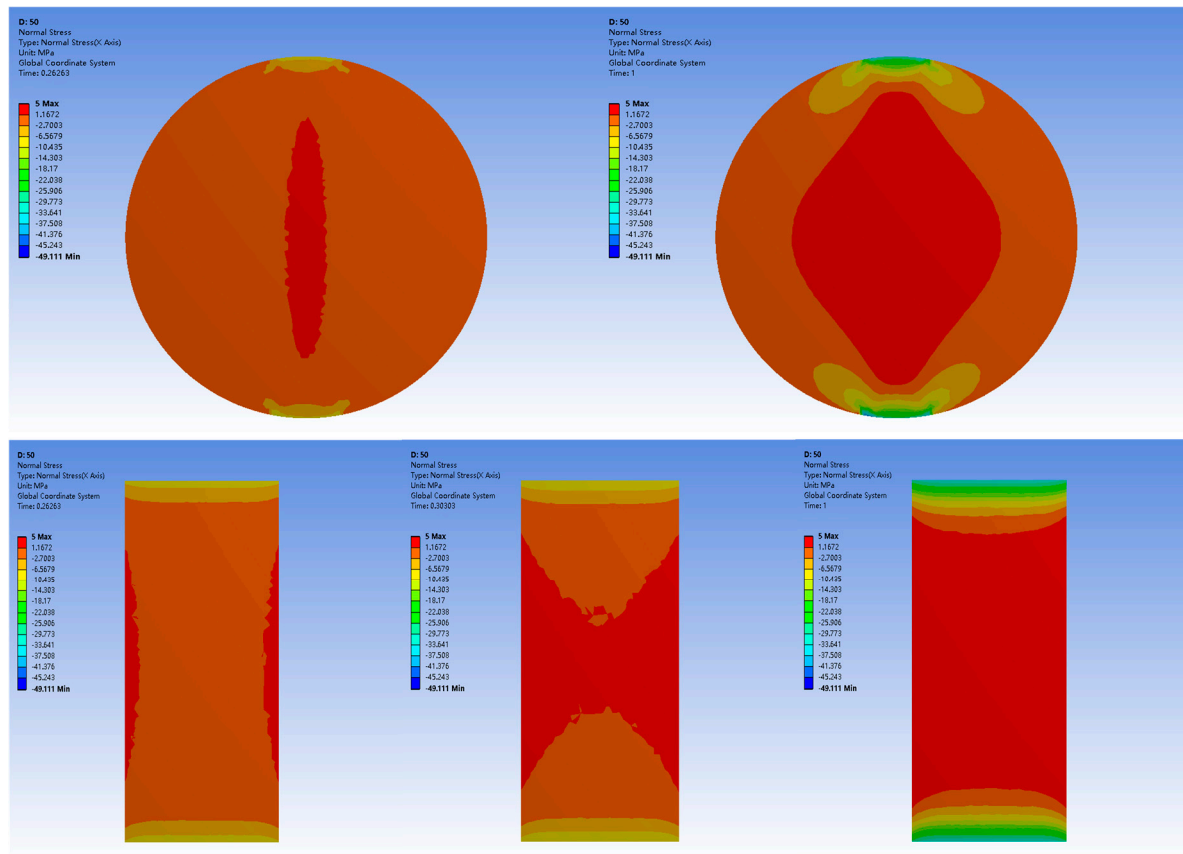
Figure 6. Disc stress distribution contour map.

Figure 7 presents a line chart comparing the tensile strength data obtained from the disc-splitting numerical simulation test with the actual tensile strength values of the specimen. It can be seen that, with the height−to−diameter ratio fixed at 2.0, the tensile strength of the specimen decreases as the disc diameter increases. In addition, there is a slight discrepancy between the tensile strength values measured in the disc-splitting test and the specimen's actual tensile strength values.

In these numerical simulation tests, two dumbbell-shaped specimens were used, both subjected to direct tensile loading at both ends. The main difference lies in the shape and angle of the transition region between the central effective test area and the two end grips. Consequently, these two dumbbell-shaped specimens were considered as one type for the purpose of analysis. Figures 8 and 9 illustrate the X-Z cross-sectional stress distribution contours at three different time points, as well as the final fracture results, for dumbbell-shaped specimens featuring an arc transition and a straight transition with a 63° inclination under a load applied along the positive Z-axis. It can be observed that, during tensile loading, the zone of maximum tensile stress first appears at the junction between the arc

transition and the central effective test area. The stress concentration then propagates in an X-shaped pattern toward the specimen's centre, ultimately forming crescent-shaped stress concentration zones on both sides of the central effective test region. From a three-dimensional perspective, these zones manifest as bowl-shaped areas of maximum tensile stress on either side. As shown in the final fracture images, the specimen's fracture surface is ultimately bowl-shaped. In actual tests, taking into account errors arising from specimen fabrication and load application, the real fracture surface tends to be a slightly raised plane, as illustrated in Figures 8d and 9d.
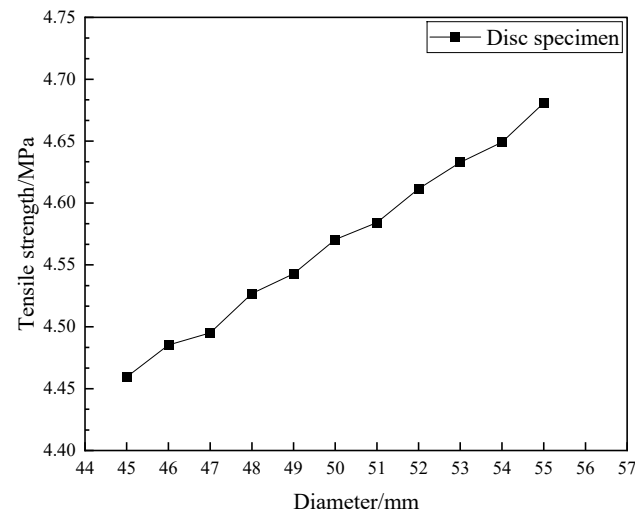

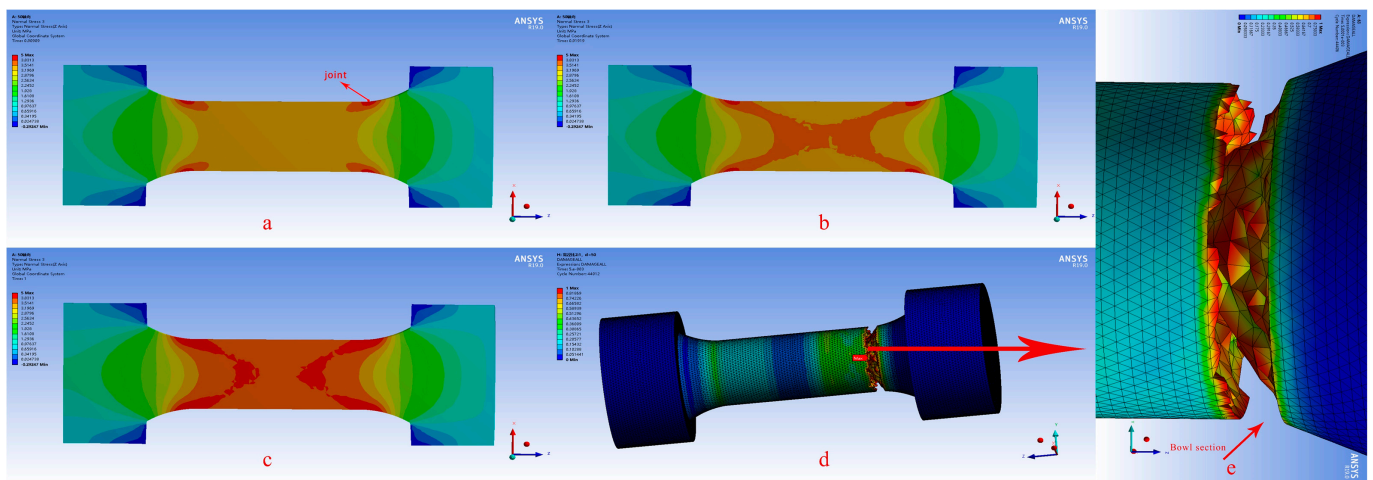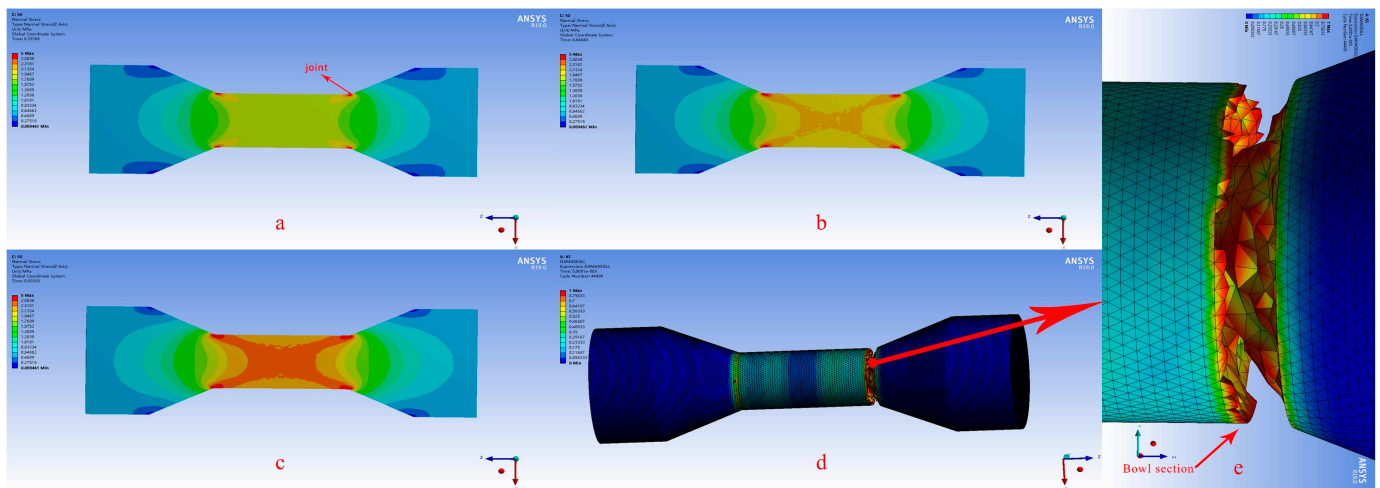**Figure 7.** The relationship between splitting tensile strength and diameter.

Figure 8. Stress distribution diagram of curved dumbbell specimen. Panels (**a**–**d**) show the stress distribution contour changes at different time points, while (**e**) shows the final fracture result.

A line chart of the tensile strength values obtained from the numerical simulation tests for both types of dumbbell-shaped specimens is presented in Figure 10. It can be seen that for specimens with an arc transition, the measured tensile strength shows a certain discrepancy compared to the actual tensile strength, whereas specimens with a straight transition exhibit a larger deviation. Meanwhile, as the diameter of the central test region increases, the measured tensile strength values for both dumbbell-shaped specimens show a slight downward trend.

Figure 9. Stress distribution diagram of straight dumbbell specimen. Panels (**a**–**d**) show the stress distribution contour changes at different time points, while (**e**) shows the final fracture result.
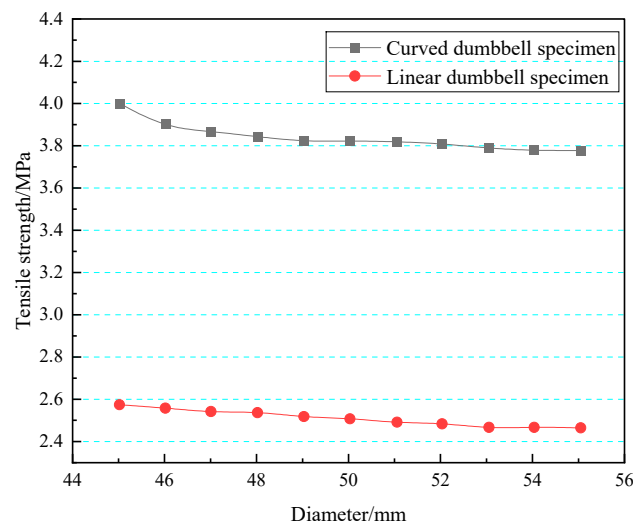
Figure 10. The relationship between the direct tensile strength and diameter of dumbbell specimens.

4. Accuracy Analysis of Diameter Correction Factor and Test Method

4.1. Diameter Correction Factor

From the above analysis, for the same rock material but differently shaped specimens, the tensile strength initially decreases and then gradually stabilizes as the specimen diameter increases, reflecting the size effect related to diameter. In engineering practice, the diameter of the cored rock depends on the drill bit size; thus, not all rock cores measure 50 mm [35]. Consequently, if non-standard-sized specimens are used for tensile strength testing, the results must be corrected. Here, the ratio of the measured strength from the splitting numerical simulation test to the preset material strength is adopted as the correction factor. After curve fitting, the formula for the correction factor k in the disc-splitting test is derived, as shown in Equation (2):

$$k_{Disc} = 0.899\,7D^{0.052\,7} \tag{2}$$

The formula is used to modify the data of the field splitting test, and the results are shown in Figure 11.
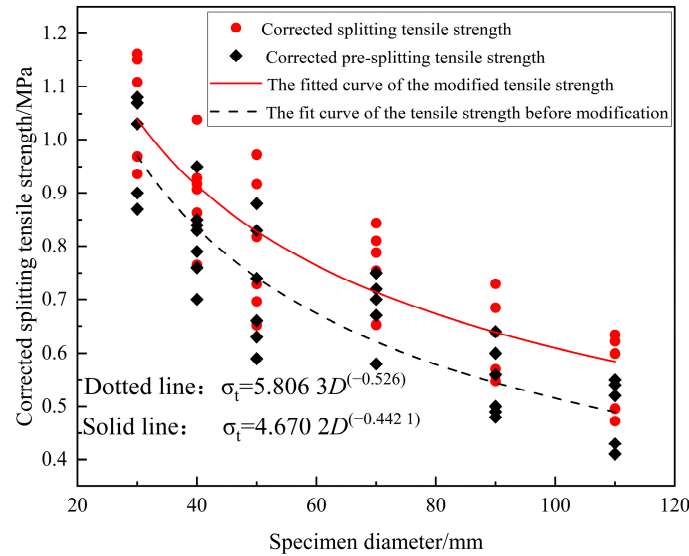
Figure 11. The relationship between split tensile strength and diameter after correction.

It can be observed that the slope of the fitted curve describing the relationship between the corrected splitting tensile strength and diameter decreases and becomes smoother. This indicates that the correction reduces the influence of diameter on the splitting tensile strength. Similarly, the correction factors for the diameters of the other two types of specimens can be obtained through curve fitting, as shown in Equations (3) and (4).

$$k_{\text{Curved dumbbell}} = 0.537\ 2D^{0.227\ 3} \tag{3}$$

$$k_{\text{Straight dumbbell}} = 0.760\ 8D^{0.246\ 8} \tag{4}$$

4.2. Analysis of the Accuracy of the Test Method

Whether it is the direct tensile test of a standard cylindrical specimen, the splitting test of a disc specimen, or the direct tensile test of a dumbbell-shaped specimen, the objective is to measure the tensile strength of rocks more accurately. However, due to the different mechanical mechanisms involved, the precision of each test varies. Therefore, analyzing the accuracy of tensile strength values obtained from different specimen shapes is crucial for accurately determining the mechanical parameters of rocks.

Figure 12 presents a comparison chart of the tensile strength test values obtained from several different specimen shapes in the numerical simulation tests and the standard tensile strength values of rocks. The line chart shows that the tensile strength test values obtained by different testing methods exhibit significant discrepancies when compared with the standard values. The tensile strength obtained from splitting tests using disc specimens shows a slight deviation from the actual tensile strength, with a discrepancy of 8.9%, as shown in Table 5. Moreover, it is more accurate compared to the tensile strength values measured from the two dumbbell-shaped specimens. However, the test results are significantly affected by the diameter of the disc specimen. The tensile strength obtained from direct tensile tests using arc-transition dumbbell-shaped specimens has a certain error compared to the actual tensile strength, with a discrepancy of 23.4%, as shown in Table 5. However, the results for these specimens are less affected by the diameter of the central effective test area, with the tensile strength values remaining relatively stable regardless of the diameter variation in the central test region. The tensile strength obtained from tests using straight-transition dumbbell-shaped specimens also remains relatively stable.

However, it shows a significant deviation from the actual tensile strength, with an error reaching 49.9%, as shown in Table 5.
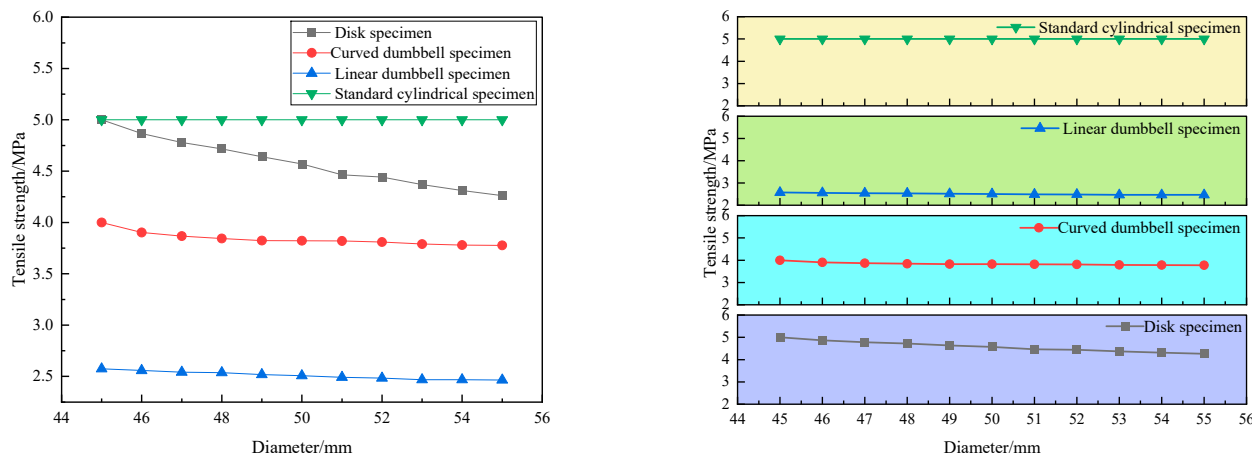

Figure 12. Comparison of measured tensile strength of different specimens.

Table 5. Deviation of tensile strength measured by different specimens.

Specimen Shape	Deviation/%
Standard cylinder	0
disc	8.90
Curved-transition plane dumbbell shape	23.40
Straight-transition plane dumbbell shape	49.90

This is primarily because, during the loading of a dumbbell-shaped specimen with a linear transition, a significant stress concentration can form at the transition region near the specimen's root. This stress concentration may lead to early failure at that location, resulting in a lower measured tensile strength. This phenomenon is especially pronounced in brittle rocks, where a linear-transition shape facilitates crack propagation at stress concentration sites, eventually causing fracture. By contrast, in a dumbbell-shaped specimen with a curved transition, the smooth contour helps distribute the applied tensile stress more evenly, reducing the likelihood of stress concentration. Consequently, cracks typically initiate in the central region of the specimen and spread uniformly, resulting in a more stable fracture pattern. This design thus provides test values closer to the material's true tensile strength. Due to stress concentration, dumbbell-shaped specimens with a linear transition may fail earlier, typically yielding lower tensile strength values. In contrast, dumbbell-shaped specimens with a curved transition generally exhibit slightly higher tensile strength values, thanks to improved stress distribution, and their test results are more consistent and reliable. A linear-transition dumbbell-shaped specimen can be considered a simplified version of the curved-transition specimen, replacing the rounded corners with oblique straight lines. Consequently, in terms of testing accuracy, the curved-transition design outperforms the linear-transition design [36–38].

Further analysis shows that under the condition of isotropic rock, compared to direct tension, the disc specimen, with its regular shape, easily controlled force boundaries, and good alignment, can more easily achieve a concentrated and stable tensile failure zone under the same testing conditions, with a more uniform stress distribution. The tensile strength measured by the Brazilian disc-splitting method is closer to the true tensile strength, thereby confirming the advantages of the disc specimen in engineering practice [39,40].

5. Conclusions

By conducting indoor splitting tests on disc specimens with different diameters but the same thickness-to-diameter ratio cast simultaneously, and performing numerical simulations of tensile strength on three different specimen shapes made of the same material, the following conclusions are drawn:

(1) In the laboratory splitting tests, the measured tensile strength decreases with an increase in the diameter of the disc specimens and then stabilizes. This variation can be well fitted using an exponential function. The results of this splitting test can be accurately fitted using the power function $\sigma t = 5.806\ 3D^{-0.526}$. Additionally, numerical simulations indicate that the tensile strength obtained from disc-splitting tests is less than the actual tensile strength. For field tests, it is recommended to multiply the results by a coefficient, with the correlation coefficient suggested as 1.089 based on the numerical simulations.

(2) For dumbbell-shaped specimens, the tensile strength measured from direct tensile tests shows a slight decrease as the diameter of the central effective test area decreases. The measured tensile strength is also lower than the actual tensile strength. For field tests, the use of straight−transition dumbbell-shaped specimens is not recommended due to significant deviation. If arc-transition dumbbell-shaped specimens are used for direct tensile tests, it is recommended to multiply the results by a coefficient, with the correlation coefficient suggested as 1.234 based on the numerical simulations.

(3) Compared to dumbbell-shaped specimens, the results from disc specimens are closer to the actual tensile strength of rocks. Additionally, disc specimens are easier to fabricate and more suitable for construction sites, whereas dumbbell-shaped specimens, which require machining on a lathe, are more appropriate for laboratory comparative studies. However, in field tests, both specimen types may develop microcracks during fabrication, which could lead to deviations in the final test results.

Author Contributions: Data analysis and writing, J.P.; writing—review and editing, J.Z.; funding acquisition, S.N. All authors have read and agreed to the published version of the manuscript.

Institutional Review Board Statement: Not applicable.

Informed Consent Statement: Not applicable.

Data Availability Statement: The original contributions presented in this study are included in the article. Further inquiries can be directed to the corresponding author.

Conflicts of Interest: The authors declare no conflicts of interest.

References

1. Diederichs, M.; Kaiser, P. Tensile strength and abutment relaxation as failure control mechanisms in underground excavations. *Int. J. Rock Mech. Min. Sci.* **1999**, *36*, 69–96. [CrossRef]
2. Perras, M.A.; Diederichs, M.S. A Review of the Tensile Strength of Rock: Concepts and Testing. *Geotech. Geol. Eng.* **2014**, *32*, 525–546. [CrossRef]
3. Gao, W.; Chen, X.; Hu, C.; Zhou, C.; Cui, S. New damage evolution model of rock material. *Appl. Math. Model.* **2020**, *86*, 207–224. [CrossRef]
4. Bahaaddini, M.; Serati, M.; Masoumi, H.; Rahimi, E. Numerical assessment of rupture mechanisms in Brazilian test of brittle materials. *Int. J. Solids Struct.* **2019**, *180–181*, 1–12. [CrossRef]
5. Pandey, P.; Singh, D.P. Deformation of a rock in different tensile tests. *Eng. Geol.* **1986**, *22*, 281–292. [CrossRef]
6. Liu, J.; Lyu, C.; Lu, G.; Shi, X.; Li, H.; Liang, C.; Deng, C. Evaluating a new method for direct testing of rock tensile strength. *Int. J. Rock Mech. Min. Sci.* **2022**, *160*, 105258. [CrossRef]

7. Wu, Y.; Liu, J.; Wu, Z.; Liu, J.; Zhao, Y.; Xu, H.; Wei, J.; Zhong, W. A universal direct tensile testing method for measuring the tensile strength of rocks. *Int. J. Min. Sci. Technol.* **2024**, *34*, 1443–1451. [CrossRef]

8. Liao, Z.Y.; Zhu, J.B.; Tang, B.C.A. Numerical investigation of rock tensile strength determined by direct tension, Brazilian and three-point bending tests. *Int. J. Rock Mech. Min. Sci.* **2019**, *115*, 21–32. [CrossRef]

9. Komurlu, E.; Demir, S. Determination of Direct Tensile Strength Values of Rock Materials by a New Test Method of Drilled Disc Tension. *Period. Polytech.-Civ. Eng.* **2020**, *64*, 33–41. [CrossRef]

10. Aliha, M.R.M.; Ebneabbasi, P.; Karimi, H.r.; Nikbakht, E. A novel test device for the direct measurement of tensile strength of rock using ring shape sample. *Int. J. Rock Mech. Min. Sci.* **2021**, *139*, 104649. [CrossRef]

11. Perras, M.A.; Diederichs, M.S. Predicting excavation damage zone depths in brittle rocks. *J. Rock Mech. Geotech. Eng.* **2016**, *8*, 60–74. [CrossRef]

12. Vogler, D.; Walsh, S.D.C.; Dombrovski, E.; Perras, M.A. A comparison of tensile failure in 3D-printed and natural sandstone. *Eng. Geol.* **2017**, *226*, 221–235. [CrossRef]

13. Komurlu, E.; Kesimal, A.; Demir, A.D. Dog bone shaped specimen testing method to evaluate tensile strength of rock materials. *Geomech. Eng.* **2017**, *12*, 883–898. [CrossRef]

14. Huang, Y.; Wang, L.; Chen, J.; Zhang, J. Theoretical analysis of rock tensile strength determined by Brazilian splitting test of platform. *Rock Soil Mech.* **2015**, *36*, 739–748. [CrossRef]

15. You, M.; Su, C. Experimental study on split test with flattened disk and tensile strength of rock. *Chin. J. Rock Mech. Eng.* **2004**, *18*, 3106–3112. (In Chinese)

16. You, M.; Su, C. Theory and experiment of platform disc splitting. *Chin. J. Rock Mech. Eng.* **2004**, *01*, 170–174. (In Chinese)

17. Guo, T.; Wang, H.; Si, X.; Pu, C.; Liu, Z.; Zhang, Q.; Liu, W. Fracture Characteristics and Tensile Strength Prediction of Rock–Concrete Composite Discs Under Radial Compression. *Mathematics* **2024**, *12*, 3510. [CrossRef]

18. *GB/T 50266-2013*; Standard for Test Methods for Engineering Rock Mass. Ministry of Housing and Urban-Rural Development of the People's Republic of China: Chengdu, China, 2023. (In Chinese)

19. Dou, F.; Hou, P.; Jia, Z.; Wang, C.; Zhao, H.; Wang, Y. Effect of clay minerals on tensile failure characteristics of shale. *ACS Omega* **2022**, *7*, 24219–24230. [CrossRef]

20. *ASTM D3967-16*; Standard Test Method for Splitting Tensile Strength of Intact Rock Core Specimens. ASTM: West Conshohocken, PA, USA, 2016. (In Chinese)

21. ISRM. Suggested Methods for Determining Tensile Strength of Rock Materials. *Int. J. Rock Mech. Min. Sci.* **1978**, *15*, 99–103. [CrossRef]

22. Komurlu, E.; Kesimal, A.; Demir, S. Experimental and numerical study on determination of indirect (splitting) tensile strength of rocks under various load apparatus. *Can. Geotech. J.* **2015**, *53*, 360–372. [CrossRef]

23. Xu, Y.; Yao, W.; Xia, K. Numerical study on tensile failures of heterogeneous rocks. *J. Rock Mech. Geotech. Eng.* **2020**, *12*, 50–58. [CrossRef]

24. *DL/T 5368-2007*; Regulations for Rock Tests of Hydropower and Water Conservancy Projects. Ministry of Water Resources of the People's Republic of China: Chengdu, China, 2007. (In Chinese)

25. Komurlu, E. Loading rate conditions and specimen size effect on strength and deformability of rock materials under uniaxial compression. *Int. J. Geo-Eng.* **2018**, *9*, 17. [CrossRef]

26. Briševac, Z.; Kujundžić, T.; Čajić, S. Current Cognition of Rock Tensile Strength Testing By Brazilian Test. *Min.-Geol.-Pet. Eng. Bull.* **2015**, *30*, 101–114. [CrossRef]

27. Demirdag, S.; Tufekci, K.; Sengun, N.; Efe, T.; Altindag, R. Determination of the Direct Tensile Strength of Granite Rock by Using a New Dumbbell Shape and its Relationship with Brazilian Tensile Strength. *IOP Conf. Ser.-Earth Environ. Sci.* **2018**, *221*, 012094. [CrossRef]

28. Zhang, S.; Lu, Y.B. Experimental and numerical investigation on the dumbbell-shaped specimen of concrete-like materials under tension. *Lat. Am. J. Solids Struct.* **2018**, *15*, e93. [CrossRef]

29. Lin, H.; Xiong, W.; Yan, Q. Three-Dimensional Effect of Tensile Strength in the Standard Brazilian Test Considering Contact Length. *Geotech. Test. J.* **2016**, *39*, 137–143. [CrossRef]

30. Li, D.; Wong, L.N.Y. The Brazilian Disc Test for Rock Mechanics Applications: Review and New Insights. *Rock Mech. Rock Eng.* **2013**, *46*, 269–287. [CrossRef]

31. Kourkoulis, S.; Markides, C.F.; Chatzistergos, P. The standardized Brazilian disc test as a contact problem. *Int. J. Rock Mech. Min. Sci.* **2013**, *57*, 132–141. [CrossRef]

32. Markides, C.F.; Kourkoulis, S. The stress field in a standardized Brazilian disc: The influence of the loading type acting on the actual contact length. *Rock Mech. Rock Eng.* **2012**, *45*, 145–158. [CrossRef]

33. Japaridze, L. Stress-deformed state of cylindrical specimens during indirect tensile strength testing. *J. Rock Mech. Geotech. Eng.* **2015**, *7*, 509–518. [CrossRef]

34. Tang, H.; He, J.; Gan, Z.; Li, J.; Hua, W.; Dong, S. Tensile strength and elastic modulus determined in the Brazilian test: Theory and experiment. *Meccanica* **2022**, *57*, 2533–2552. [CrossRef]

35. Feng, L.A.; Jasiuk, I. Effect of specimen geometry on tensile strength of cortical bone. *J. Biomed. Mater. Res. Part A* **2010**, *95A*, 580–587. [CrossRef] [PubMed]

36. Wang, C.; Xia, Y. Three-dimensional Analysis of Bar-Bar Tensile Impact Testing Apparatus with a Flat Specimen by Elastoplastic FEM. *Chin. J. Appl. Mech.* **2000**, *17*, 121–126. (In Chinese)

37. Wang, C.; Xia, Y. Two Dimensional Axisymmetric Analysis of Bar Bar Tensile Impact Testing Apparatus by Elastoplastic FEM. *Chin. J. Appl. Mech.* **1999**, *16*, 65–73. (In Chinese)

38. Wang, C.; Wan, H.; Xia, Y. A Two-Dimensional Axisymmetric Numerical Analysis of a Bar–Bar Tensile Impact Apparatus by Elastoplastic Fem. *J. Sound Vib.* **1999**, *220*, 787–806. [CrossRef]

39. Mellor, M.; Hawkes, I. Measurement of tensile strength by diametral compression of discs and annuli. *Eng. Geol.* **1971**, *5*, 173–225. [CrossRef]

40. Fairhurst, C. On the validity of the 'Brazilian' test for brittle materials. *Int. J. Rock Mech. Min. Sci. Geomech. Abstr.* **1964**, *1*, 535–546. [CrossRef]